Catena 194 (2020) 104722

Contents lists available at ScienceDirect

Catena

journal homepage: www.elsevier.com/locate/catena

Changes of soil organic carbon stocks from the 1980s to 2018 in northern China's agro-pastoral ecotone

Xuyang Wang[a,b], Yuqiang Li[a,c,*], Xiangwen Gong[d], Yayi Niu[a,b], Yinping Chen[e], Xiaoping Shi[e], Wei Li[f], Jing Liu[a]

[a] Northwest Institute of Eco-Environment and Resources, Chinese Academy of Sciences, Lanzhou 730000, China
[b] University of Chinese Academy of Sciences, Beijing 100049, China
[c] Naiman Desertification Research Station, Northwest Institute of Eco-Environment and Resources, Chinese Academy of Sciences, Tongliao 028300, China
[d] Wan Sheng Mining of Chongqing Conservation and Repair of Ecological Environment Observation and Research Station, Chongqing Institute of Geology and Mineral Resources, Chongqing 400042, China
[e] School of Environmental and Municipal Engineering, Lanzhou Jiaotong University, Lanzhou 730070, China
[f] Northwest Agriculture and Forestry University, Yangling 712100, Shaanxi, China

ARTICLE INFO

Keywords:
Soil organic carbon (SOC)
Total SOC stock
Climate change
Land use/cover change
Agro-pastoral ecotone

ABSTRACT

Soil carbon sequestration and potential sequestration are key issues in global carbon research, as the size of the soil organic carbon (SOC) stocks and their changes over time are important for understanding their role in climate change. In northern China's agro-pastoral ecotone, we compared SOC data derived from 238 sampling sites during China's National Soil Inventory in the 1980s with the results of field surveys at 644 sites in 2018 to calculate the changes in SOC stocks between the 1980s and 2018. We found that the mean SOC stock to a depth of 30 cm decreased significantly, from 4.48 kg C m^{-2} in the 1980s to 3.60 kg C m^{-2} in 2018, and the total SOC stock decreased from 2793.17 Tg to 2248.34 Tg. This amounted to an average decrease of 27.74 g C m^{-2} yr^{-1} over the 30-year study period. Furthermore, we used a land use and cover change transition matrix to quantify the amount of SOC change caused by these transitions; the SOC reduction could be mainly ascribed to overgrazing, grassland reclamation for agriculture, and grassland desertification. Large-scale ecological restoration projects have increased SOC reserves, but not enough to compensate for the loss of SOC caused by factors such as desertification and ecosystem degradation. We also performed regression analysis for the relationship between the change in the SOC stock and the rates of temperature and precipitation change. We found that increasing temperature non-significantly decreased SOC, whereas precipitation was significantly ($P < 0.05$) related to SOC change, but the R^2 was very low (0.01). Our analysis suggests that humans have affected SOC in northern China's agro-pastoral ecotone more strongly than climatic factors.

1. Introduction

Soil is the largest carbon pool in terrestrial ecosystems. About 1400 to 1500 Pg carbon is stored in the soil in the form of organic matter, accounting for two-thirds to three-quarters of the total carbon pool in terrestrial ecosystems (Post et al., 1982; Schlesinger, 1990). Due to the soil's huge capacity to store soil organic carbon (SOC), even a slight change in SOC pools could significantly influence the atmospheric carbon dioxide (CO_2) concentration, which in turn will affect global climate change (Were et al., 2015). The massive global emissions of greenhouse gases such as CO_2 have become the main cause of global warming since the mid-20th century, and changes in SOC pools have huge potential for mitigating or exacerbating atmospheric levels of greenhouse gases (Davidson and Janssens, 2006; Novaes et al., 2017; Raich and Potter, 1995). Hence, many scholars have studied the relationship between SOC dynamics and atmospheric CO_2 accumulation (Jobbagy and Jackson, 2000; Smith et al., 2008; Valtera and Šamonil, 2018; Wang et al., 2018).

Under the United Nations Framework Convention on Climate Change, soil carbon sequestration plays an important role in decreasing levels of atmospheric CO_2, thereby mitigating global warming (Ingram and Fernandes, 2001; Schlesinger, 2001). Precise estimates of the SOC stock are required to evaluate potential sequestration. Therefore, research has been performed on the spatial patterns and stocks of SOC at

* Corresponding author at: Northwest Institute of Eco-Environment and Resources, Chinese Academy of Sciences, 320 Donggang West Road, Lanzhou 730000, China.
E-mail address: liyq@lzb.ac.cn (Y. Li).

https://doi.org/10.1016/j.catena.2020.104722
Received 11 October 2019; Received in revised form 5 May 2020; Accepted 29 May 2020

a global scale (Batjes, 2014; Eswaran et al., 1993; Scharlemann et al., 2014; Tashi et al., 2016). This research has also been conducted at regional and national scales, such as in North and South America (Batjes, 2000), Brazil (Bernoux et al., 2002), France (Arrouays et al., 2010; Martin et al., 2014), Denmark (Krogh et al., 2003), India (Bhattacharyya et al., 2000), Japan (Matsuura et al., 2012), and China (Yang et al., 2007), as well as at subnational scales (Gelaw et al., 2014; Li et al., 2018; Sheikh et al., 2009). However, these studies mainly focused on the spatial distribution and stocks of SOC during a limited period. Long-term studies of SOC dynamics at large (regional or national) scales are rare, so these dynamics are poorly understood. Such research would require high sampling densities and sufficiently long time periods to observe SOC changes despite the large spatial variation of this parameter and its slow rates of change (Minasny et al., 2011). Unfortunately, achieving a high sampling density is expensive and time-consuming. Thus, monitoring of SOC dynamics has been limited to studies based on long-term trials with low sampling intensity and small spatial extent (Smith et al., 1997).

It is possible to study large-scale SOC dynamics in countries or regions with a rich monitoring infrastructure, such as Germany (Capriel, 2013), France (Arrouays et al., 2002), and the United Kingdom (Bellamy et al., 2005a, 2005b). Based on SOC data derived from China's National Soil Inventory during the 1980s, Yang et al. (2009, 2010a,2010b) conducted soil surveys in the grasslands of Tibet and northern China from 2001 to 2005 to detect the changes in the SOC stock since the 1980s, and found that grassland SOC stocks remained relatively stable during the two decades before their study. Similarly, Dai et al. (2014) estimated that the SOC stock increased by 7.00 g $C{\cdot}m^{-2}{\cdot}yr^{-1}$ in the grasslands of Inner Mongolia from the 1980s to the 2010s, but the change was not statistically significant. In contrast, Chen et al. (2017) found a significant increase at a rate of 4.66 g $C{\cdot}m^{-2}{\cdot}yr^{-1}$ from 2002 to 2011 in the SOC stocks of Tibetan grasslands. However, these estimates were limited to grasslands rather than a range of ecosystems. A comprehensive assessment of SOC dynamics in a large geographical area that includes a variety of land use and cover types has not yet been performed in China. Fortunately, China's National Soil Inventory in the 1980s provides a strong basis on which to perform such an assessment and detect changes in the subsequent 30–40 years.

Researchers consider climate and human activity (e.g., cultivation, grazing, afforestation) to be the two major groups of factors that affect SOC. Large amounts of SOC can be sequestered through afforestation, as well as by conversion of cultivated land to grassland and by controlling desertification. In contrast, SOC stocks will decrease during desertification or the conversion of a natural landscape into intensively managed cropland (Gelaw et al., 2014; Lal, 2001). Temperature and precipitation control the balance between carbon inputs from plant residues and carbon outputs through their effects on plant growth and on decomposition of SOC by soil microorganisms (Post et al., 1982). The effects of climate on SOC have been well characterized in recent years, and researchers have generally found that SOC was negatively correlated with temperature and positively correlated with precipitation (Chen et al., 2017; Davidson and Janssens, 2006; Jobbagy and Jackson, 2000; Smith et al., 2008).

Lal (2004) reported that 78 ± 12 Pg C were contributed to the atmosphere since the industrial revolution by depletion of the global SOC pool, mainly caused by unreasonable land use practices, including cultivation, deforestation, conversion of natural to agricultural ecosystems, and biomass burning, whereas the global potential SOC sequestration rate could reach 0.9 ± 0.3 Pg C yr^{-1} if restorative land use practices and improved management practices were implemented. Bellamy et al., 2005a, 2005b) and Yang et al. (2009) suggested that climate warming may lead to a loss of soil carbon based on their analysis of numerous findings from small-scale laboratory incubations, field experiments, and modeling studies. However, little evidence has been available from large-scale observations based on soil inventory data (Yang et al., 2009). Bell et al. (2011) found that the UK's soils sequester a total of 102 Tg C, and that sequestration has benefited from an increase in the area of woodland, from conversion of arable land into permanent grassland from 1925 to 2007, and from the SOC gains that resulted from land-use change that offset losses caused by climate change. Deng and Shangguan (2017) found that SOC to a depth of 100 cm increased at 0.23 g kg^{-1} yr^{-1} following afforestation based on compilation and analysis of published data from 512 observations at 61 sites in China.

Northern China's agro-pastoral ecotone is a typical ecologically fragile semi-arid zone that has undergone severe desertification. The ecosystem degradation has been caused by natural factors, such as a dry climate (high rates of evaporation), inadequate precipitation, and strong winds. These factors have been exacerbated by intensive cultivation and overgrazing over large areas (Wang et al., 2019). For example, in the agro-pastoral ecotone of Inner Mongolia Autonomous Region, the degraded grassland covered 2.1×10^5 km^2 in 1983, and this increased to 3.9×10^5 km^2 in 1995, representing an increase (linear) of about 7% per year (Zhao et al., 2002). To mitigate these problems, the government has implemented a range of restoration projects since 1975, including the Ecological Compensation Mechanism (Wan et al., 2005), the Three Norths Shelter Forest Program (Wang et al., 2010), and other grassland protection policies. However, even though the region remains highly ecologically fragile, it has high potential as a carbon sink (Nosetto et al., 2006). Thus it has become a region of interest for evaluating the effects of desertification control and the carbon sequestration potential of degraded ecosystems through strategies such as grazing exclusion (Su et al., 2003) and afforestation (Li et al., 2013, 2017; Zhang et al., 2004). However, no research has quantified the long-term SOC changes for the whole region, and there is little knowledge of the region's SOC dynamics or of how climatic and anthropogenic factors have affected the long-term SOC changes.

To provide some of the missing knowledge, we developed the present study to describe the changes that have occurred since the 1980s National Soil Survey. Our specific objectives were to (1) evaluate the current total SOC stock in northern China's agro-pastoral ecotone, (2) detect changes in the total SOC stock between the 1980s and 2018 in the study area at site and regional scales, and (3) analyze the effects of climatic and anthropogenic factors on SOC changes during the last 30–40 years.

2. Materials and methods

2.1. Study area

Northern China's agro-pastoral ecotone is a transitional zone in which agricultural cultivation and grazing are interlaced with natural grasslands and deserts. It lies in the ecological transition zone between the eastern farming and northwestern pastoral areas of northern China. The study area covers nine provinces with an area of 654 564 km^2, and the Inner Mongolia Autonomous Region accounts for the largest proportion (61.4%) of the total study area (Fig. 1a). The study area ranges between 36°01′N and 51°36′N and between 105°45′E and 128°42′E (Fig. 1b). The eastern section is more than 300 km wide, and includes the foothills of the Daxing'anling Forest Region, the Hulunbeier grassland, and the Horqin Sandy Land. The middle of the study area is about 200 km wide, and includes the Hunshandake Sandy Land. The Mu Us Sandy Land and China's Loess Plateau occupy the southwestern section, which is 100 to 150 km wide. Long-term mean annual precipitation ranges from 300 to 450 mm, of which more than 60% falls from June to August. Due to the wide span of 15° in latitude, the mean annual temperature (*MAT*) varies greatly. *MAT* is between 6.0 and 9.0 °C in the southwestern section, but decreases to between 0 and 1.0 °C in the middle part, and then increases to between 3.0 and 7.0 °C in the northeastern region. Mean annual wind velocity is between 3.0 and 3.8 m s^{-1}, and the frequency of gales (when the wind velocity exceeds 8 m s^{-1}) ranges from 30 to 100 days annually.

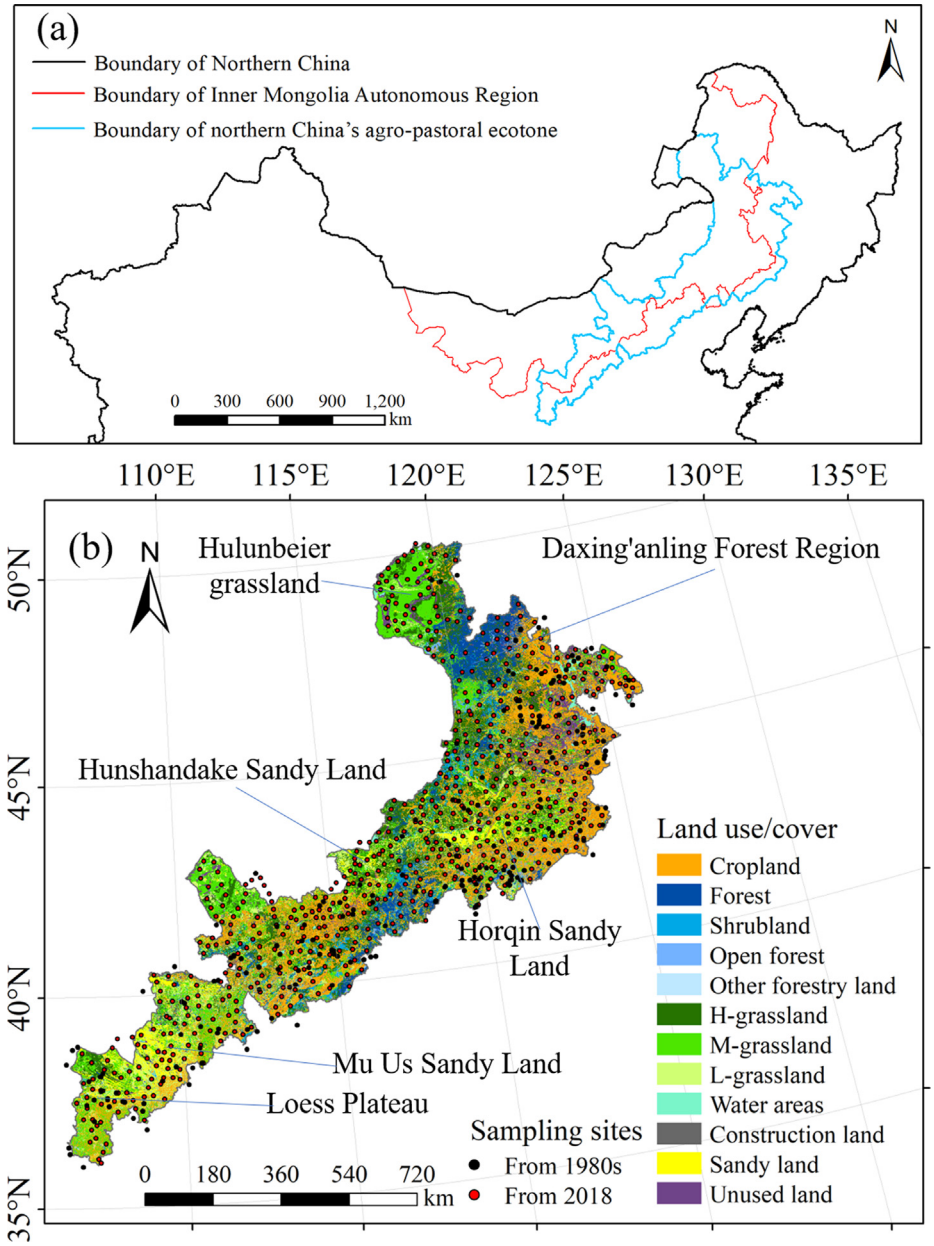

Fig. 1. (a) Locations of the Inner Mongolia Autonomous Region and the agro-pastoral ecotone of northern China. (b) Locations of the sampling sites in the agro-pastoral ecotone of northern China, and their relationships with the land use and cover types in 2015. H-grassland, M – grassland, and L-grassland refer to grassland with high, medium, and low vegetation cover (more than 50%, 20% to 50%, and 5% to 20%, respectively). The dataset was provided by the Data Center for Resources and Environmental Sciences, Chinese Academy of Sciences (http://www.resdc.cn).

2.2. National soil survey data

In China, a comprehensive National Soil Survey was carried out during the 1980s (from 1979 to 1989). Researchers collected a total of 34 411 soil profiles from 2444 counties, 312 national farms, and 44 forests throughout China. The inventory described soil chemical and physical properties for each horizon. Analyses of the samples included chemical properties (e.g., soil organic matter [*SOM*], pH, exchangeable bases), physical properties (e.g., bulk density, texture, particle size distribution), and fertility (e.g., total N, P, K) (Shi et al., 2004). In addition, the researchers recorded details of the geographic location, layer thickness, soil type, and land use or cover type for each profile.

2.3. Data acquisition for SOC and bulk density in the 1980s

To calculate the SOC stock (*SOCS*; $kg{\cdot}m^{-2}$) at the 238 sample sites in our study area that were included in the National Soil Survey during the 1980s, we used the soil properties that determine this parameter: *SOM* ($g{\cdot}kg^{-1}$), soil bulk density (*BD*; $g{\cdot}cm^{-3}$), the volume of coarse fragments > 2 mm (% of total), and the measurement depth (cm). *SOM* was converted to SOC by multiplying *SOM* by 0.58 (Pribyl, 2010). Because *BD* was not recorded for many of the profiles in the 1980s, the empirical relationship [Eq. (1), Fig. 2a] was developed between the SOC concentration to a depth of 30 cm and *BD* using measured data from our 2018 field survey, then the formula was used to calculate *BD* for the sites from the 1980s that lacked this data. The measured *BD* values in the topsoil during the 1980s was used to validate the prediction accuracy of the following model (Fig. 2a):

$$BD = 1.4955exp^{-0.013x} (R^2 = 0.705, P < 0.001) \quad (1)$$

Where x represents the SOC concentration ($g{\cdot}kg^{-1}$). Fig. 2b shows that the predicted *BD* increased linearly with the measured values and

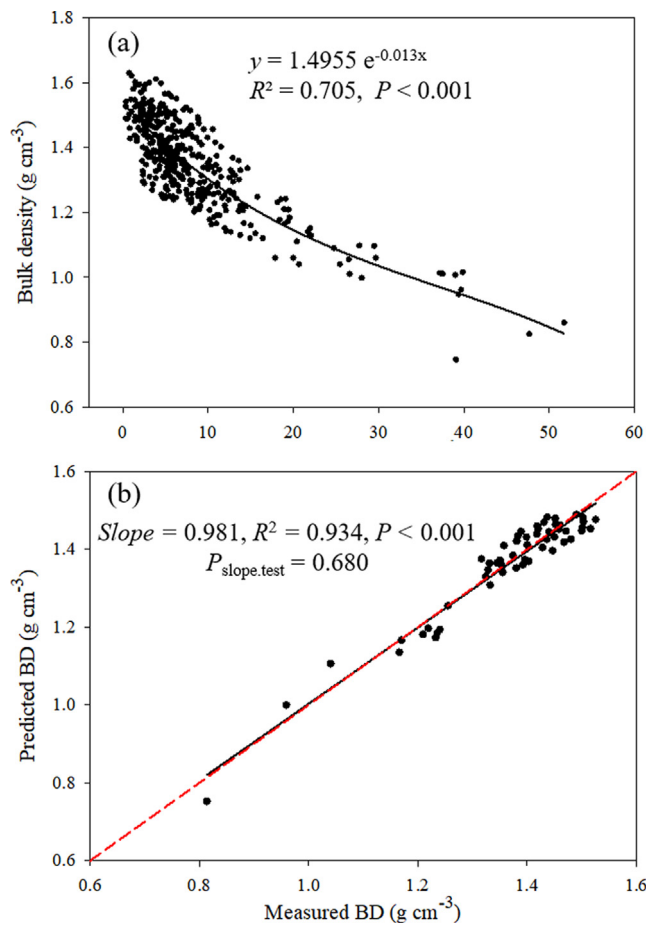

Fig. 2. Relationships between the soil organic carbon (SOC) concentration to a depth of 30 cm and bulk density (*BD*) were obtained from field measurements in 2018. (a) Development of a predictive equation for *BD* as a function of SOC. (b) To evaluate the accuracy of this empirical relationship, we used the measured BD values from the 1980s. The dashed red line represents $y = x$, and the nonsignificant *P* value for the slope test indicates that the regression slope did not differ significantly from 1.

there was no significant difference between the slope of the validation line and 1.0, suggesting that this equation provided an acceptable estimate of the missing *BD* values from the 1980 s. The box plot of *SOCS* for different land use during the 1980s is shown in Supplementary Figure S1.

2.4. Field survey and laboratory analysis in 2018

To detect changes in *SOCS* in the agro-pastoral ecotone of northern China, we obtained soil samples at 644 sites distributed throughout the study region (Fig. 1b) from April to July 2018. At each sampling site, the soil samples were collected randomly at 15 sampling locations at depths of 0 to 20 and 20 to 30 cm using a 2.5-cm-diameter soil auger. This approach agrees with the depth range used in most previous studies (Arrouays et al., 2010; Bellamy et al., 2005a, 2005b; Chen et al., 2017; Sleutel et al., 2010; Yang et al., 2009), and therefore facilitates comparison of our results with previous research. These samples were combined to produce a single composite sample at each depth, yielding a total of 1288 composite samples. In addition, three sampling points (replicates) at each site were selected to determine the soil *BD* for the 0 to 20 cm and 20 to 30 cm layers, and the samples were collected using a soil auger equipped with a stainless-steel cylinder (5.5 cm in diameter and 4.2 cm in height). Then the three *BD* values were averaged to produce a single mean value for each sampling site.

In the laboratory, the soil samples were air-dried and sieved through a 2-mm mesh to remove roots and other coarse debris. The remaining samples were then ground to pass through a 0.25-mm mesh before determination of the SOC concentration. To be consistent with the SOC measurement method used in China's National Soil Survey, the Walkley-Black dichromate oxidation method was used to determine the SOC concentration (Nelson et al., 1996). Soil *BD* was determined from the soil cores as the ratio of the oven-dry (at 105 °C) soil mass to the container volume (Klute, 1986).

2.5. Estimation of SOCS and the total stock

For the data obtained from the two soil surveys, the same method was used to calculate the SOC stock to a depth of 30 cm (*SOCS*, in kg C·m^{-2}) for each soil sample by Eq. (2), then the total *SOCS* (in Tg) was estimated from *SOCD* using Eq. (3):

$$SOCS = SOC \times BD \times D \times (1 - cf) \times 0.01 \tag{2}$$

$$Total\ SOCS = \frac{SOCS \times A}{1000} \tag{3}$$

Where *SOC* represents the elemental concentration (g C kg^{-1}), *BD* represents the soil bulk density (g·cm^{-3}), *D* represents the thickness of the layer (cm), *cf* represents the volumetric fraction occupied by coarse fragments > 2 mm (%), *A* represents the area of a given region (in km^2), and 0.01 and 1000 are unit conversion factors.

2.6. Climatic and land use data

To analyze the effects of climatic and anthropogenic factors on SOC dynamics during the study period, we obtained a gridded dataset (1 km × 1 km) for annual precipitation and mean annual air temperatures from 1980 to 2015, and interpolated values using the smoothing splines method provided by the ANUSPLIN software (Liu et al., 2008). The gridded climatic datasets were available from the Data Center for Resources and Environmental Sciences, Chinese Academy of Sciences (http://www.resdc.cn). The statistically significant changes in the annual temperature and precipitation from 1980 to 2015 were detected by the nonparametric Mann-Kendall method (Mann, 1945). The null hypothesis H_0 for these tests is that there is no trend in the series. The three alternative hypotheses are that there is a negative, non-zero, or positive trend.

The Mann-Kendall test statistic (*S*) is given by

$$S = \sum_{k=1}^{n-1} \sum_{j=k+1}^{n} Sgn(x_j - x_k) \tag{4}$$

$$Sgn(x_j - x_k) = 1 \text{ if } x_j - x_k > 0$$

$$Sgn(x_j - x_k) = 0 \text{ if } x_j - x_k = 0$$

$$Sgn(x_j - x_k) = -1 \text{ if } x_j - x_k < 0 \tag{5}$$

Where *n* is the length of the time series, *Sgn* represents the sign function (i.e., whether the value is positive, zero, or negative), and x_j and x_k represents sequential data values.

Under the null hypothesis, there is no trend in the data, and the distribution *S* is expected to have a mean of zero and a variance of

$$Var(S) = \frac{n(n-1)(2n+5)}{18} \tag{6}$$

In addition, *Z* values were calculated to indicate the trend's significance level using the following equations:

$$Z = \frac{S-1}{\sqrt{Var(S)}} \text{ if } S > 0$$

$$Z = 0 \text{ if } S = 0$$

$$Z = \frac{S+1}{\sqrt{Var(S)}} \text{ if } S < 0 \tag{7}$$

Thus, when performing a two-sided significance test, the null hypothesis H_0 would be rejected at significance level p if $|Z| \geq Z_{(1-p/2)}$. A positive value of Z represents an increasing trend, whereas a negative value indicates a decreasing trend. When the absolute value of Z is greater than or equal to 1.28, 1.64, and 2.32, the test is significant at p less than 0.10, 0.05, and 0.01, respectively.

The land use and cover raster data (1 km × 1 km) for 1980 and 2015 were available from the Data Center for Resources and Environmental Sciences, Chinese Academy of Sciences (http://www.resdc.cn). The main land uses in the study area include cropland, forest, and H-grassland, M−grassland, and L-grassland with high, medium, and low vegetation cover (i.e., more than 50%, 20% to 50%, and 5% to 20%, respectively). Furthermore, it includes small areas of sandy land, construction land, and unused land (e.g., saline land, gobi desert, marshland). To explore the changes in land use and cover type between the 1980s and 2015, the raster data from both times was used to generate a land transfer matrix (i.e., a matrix that shows the area of a given land use or cover type that changed to a different use or type) using the Spatial Analyst tool in version 10.3 of the ArcGIS for Desktop software (http://www.esri.com). In addition, the data on the annual number of livestock (cattle, sheep, and goats) in the region from 1980 to 2017 was available from the National Bureau of Statistics of China (http://www.stats.gov.cn/tjsj/).

2.7. Spatial aggregation of SOC data

To detect changes in the regional distribution of *SOCS* between the 1980s and 2018, it's necessary to define the corresponding spatial pattern of *SOCS*. To accomplish this, we used ordinary kriging interpolation in version 10.3 of the ArcMap software (http://www.esri.com), with the measured *SOCS* values in the two periods used as inputs, then this data was converted into raster datasets at a spatial resolution of 1 km × 1 km. The semi-variograms were used to quantify the spatial variation of SOC in this study:

$$r(h) = \frac{1}{2}E[z(x) - z(x+h)]^2 \tag{8}$$

Where $r(h)$ represents semivariance, E is the statistical expectation, and $z(x)$ and $z(x+h)$ represent the paired data values being compared over a lag distance of h (Allan Reese 2001). The semi-variogram includes three fitting models (exponential, spherical, and Gaussian), each of which can be described by the range, sill, and nugget parameters. To choose the optimal model, the mean standardized error (*MSE*) and the root-mean-square standardized error (*RMSSE*) were calculated:

$$MSE = \frac{\sum_{i=1}^{n}[\hat{Z}(x_i) - Z(x_i)]/\hat{\delta}(x_i)}{n} \tag{9}$$

$$RMSSE = \frac{\sum_{i=1}^{n}\{[\hat{Z}(x_i) - Z(x_i)]/\hat{\delta}(x_i)\}^2}{n} \tag{10}$$

Where n represents the sample size, $\hat{Z}(x_i)$and $Z(x_i)$represent the predicted and measured values of sample i at location x , respectively, and $\hat{\delta}(x_i)$represents the standard error of the prediction. Furthermore, the 238 sampling points from the 1980 s were used to extract the corresponding values from the 2018 raster dataset to obtain the *SOCS* values of 238 paired samples. In the same way, for the 644 sampling sites in 2018, the past values of *SOCS* were extracted from the 1980s raster dataset to provide an additional 644 paired samples. Thus, a total site-level database of 882 paired samples was established to describe *SOCS* changes at the same sampling sites. The *SOCS* of 882 samples between the two sampling periods were compared using paired *t*-tests. Statistical significance was defined at $P < 0.001$. The statistical analysis was performed using version 19.0 of the SPSS software (https://www.ibm.com/analytics/spss-statistics-software). The correlations between parameters were displayed using version 12.5 of SigmaPlot (https://systatsoftware.com/). To test the reliability of the empirical function developed by SOC concentration and *BD* measured data during 2018 field survey, the significance of the difference between the slope of the validation line and 1.0 was tested using the smatr standardized major axis regression package for the R software (R Development Core Team, 2008).

2.8. Uncertainty analysis of SOCS estimation

The uncertainties in *SOCS* estimation and comparisons between the 1980 s and 2018 for site-level database of 882 paired samples were conducted by Monte-Carlo simulation (Ogle et al., 2003; Vandenbygaart et al., 2004; Beilman et al., 2008; Yang et al., 2010a, 2010b). Specifically, we randomly extracted data of *SOCS* with bootstrapping techniques to estimate SOC stock and its changes (Potvin and Roff, 1993). We conducted 10 000 model analyses and summarized model outputs for each run. From these 10 000 estimates, we obtained the 2.5% and 97.5% as a description of uncertainty of *SOCS* and its changes (i.e., 95% confidence interval) (Ogle et al., 2003; Yang et al., 2010a, 2010b).

3. Results

3.1. Descriptive statistics

Table 1 summarizes the statistical characteristics of *SOCS* to a depth of 30 cm for the soil surveys in the 1980 s and in 2018. The mean value of *SOCS* in the 1980s (3.82 kg C·m^{-2}) was higher than that in 2018 (3.63 kg C·m^{-2}). *SOCS* was highly variable, and ranged from 0.17 to 13.48 kg C·m^{-2} in the 1980 s and from 0.16 to 18.47 in 2018. In addition, *SOCS* was positively skewed in the 1980 s and 2018 because the corresponding skewness was greater than 0; to account for this, we log-transformed the data before interpolation.

3.2. Semi-variogram analysis of SOCS

The isotropic exponential model provided the best fit for the semi-variograms in both time periods, with the *MSE* nearest to zero and *RMSSE* nearest to 1 (Table 2). The nugget was also smallest using the exponential model in the 1980s and 2018, with nugget sizes of 0.22 and 0.17, respectively. The nugget to sill ratios for *SOCS* were 56.9 and 41.8% in the 1980s and 2018, respectively, indicating that *SOCS* exhibited moderate spatial dependence based on the criteria of Cambardella et al. (1994), and the spatial dependence of *SOCS* decreased from the 1980s to 2018. The range is the distance at which the semi-variogram model reaches its limiting value (the sill). Beyond that range, the dissimilarity between points becomes constant with increasing lag distance. The range of *SOCS* in 2018 was less than that in the 1980s.

3.3. Spatial patterns of SOCS

SOCS showed generally consistent spatial patterns during the 1980s and in 2018 (Fig. 3a, b). *SOCS* increased from the southwest to the central part of the study area, decreased again towards the northeast,

Table 1
Statistical characteristics of the soil organic carbon stock (*SOCS*) for the two soil surveys in the agro-pastoral ecotone of northern China.

Year	*N*	*SOCS* (kg C m^{-2})				CV	Ske	Kur
		Mean	Min.	Max.	SD			
1980s	238	3.82	0.17	13.48	2.76	72.23%	1.27	1.14
2018	644	3.63	0.16	18.47	2.72	74.83%	1.88	4.34

N, sample size; Min., minimum; Max., maximum; SD, standard deviation; CV, coefficient of variation; Ske, skewness; Kur, kurtosis.

Table 2
Semi-variogram parameters for the spatial distribution of the soil organic carbon stock (*SOCS*) for two soil surveys in the agro-pastoral ecotone of northern China.

Years	Model	Nugget	Partial sill	Sill	Nugget/sill	Range (km)	*MSE*	*RMSSE*
1980s	Exponential	0.22	0.17	0.39	56.90%	355.80	0.02	1.08
	Spherical	0.23	0.16	0.39	59.90%	305.19	0.03	1.09
	Gaussian	0.25	0.15	0.40	62.65%	265.16	0.04	1.09
2018	Exponential	0.17	0.23	0.40	41.77%	215.48	0.09	0.95
	Spherical	0.21	0.18	0.39	54.46%	189.34	0.10	0.97
	Gaussian	0.24	0.15	0.39	62.09%	164.94	0.10	0.96

ME and *RMSSE* represent the mean standardized error and the root-mean-square standardized error, respectively.

and increased again to the north. The areas with a low value (< 2 kg C·m^{-2}) were mainly located in the Loess Plateau and Mu Us Sandy Land in the southwest, and in the Horqin Sandy Land in the east, which were dominated by degraded grasslands and severely desertified sandy land. The highest *SOCS* values (> 10 kg C·m^{-2}) were mainly found in the Hulunbeier grassland and Daxing'anling forest region in the northernmost part of the study area, which represented areas of well-preserved grassland and mountain forest. The *SOCS* change during the study period showed high spatial heterogeneity. In total, 31.2% of the pixels exhibited an increasing trend from the 1980s to 2018, but the remaining 68.8% showed a decreasing trend (Fig. 3c, d). Moreover, pixels with a decrease between 0 and 0.5 kg C m^{-2} per decade accounted for the largest proportion (46.8%) of the pixels.

Table 3
Ninety-five percent confidence intervals of SOC stock (*SOCS*) and its changes in the agro-pastoral ecotone of northern China., estimated by a Monte-Carlo simulation.

Item	Mean	Lower 2.5%	Upper 97.5%
*SOCS*1980s (kg·m^{-2})	4.27	4.06	4.49
*SOCS*2018 (kg·m^{-2})	3.49	3.30	3.67
SOC change (kg·m^{-2})	−0.79	−0.98	−0.59
Relative SOC change (%)	−18.41%	−23.04%	−13.79%

Relative SOC change is equal to SOC change divided by mean SOC stock during the two sampling periods. SOC, soil organic carbon.

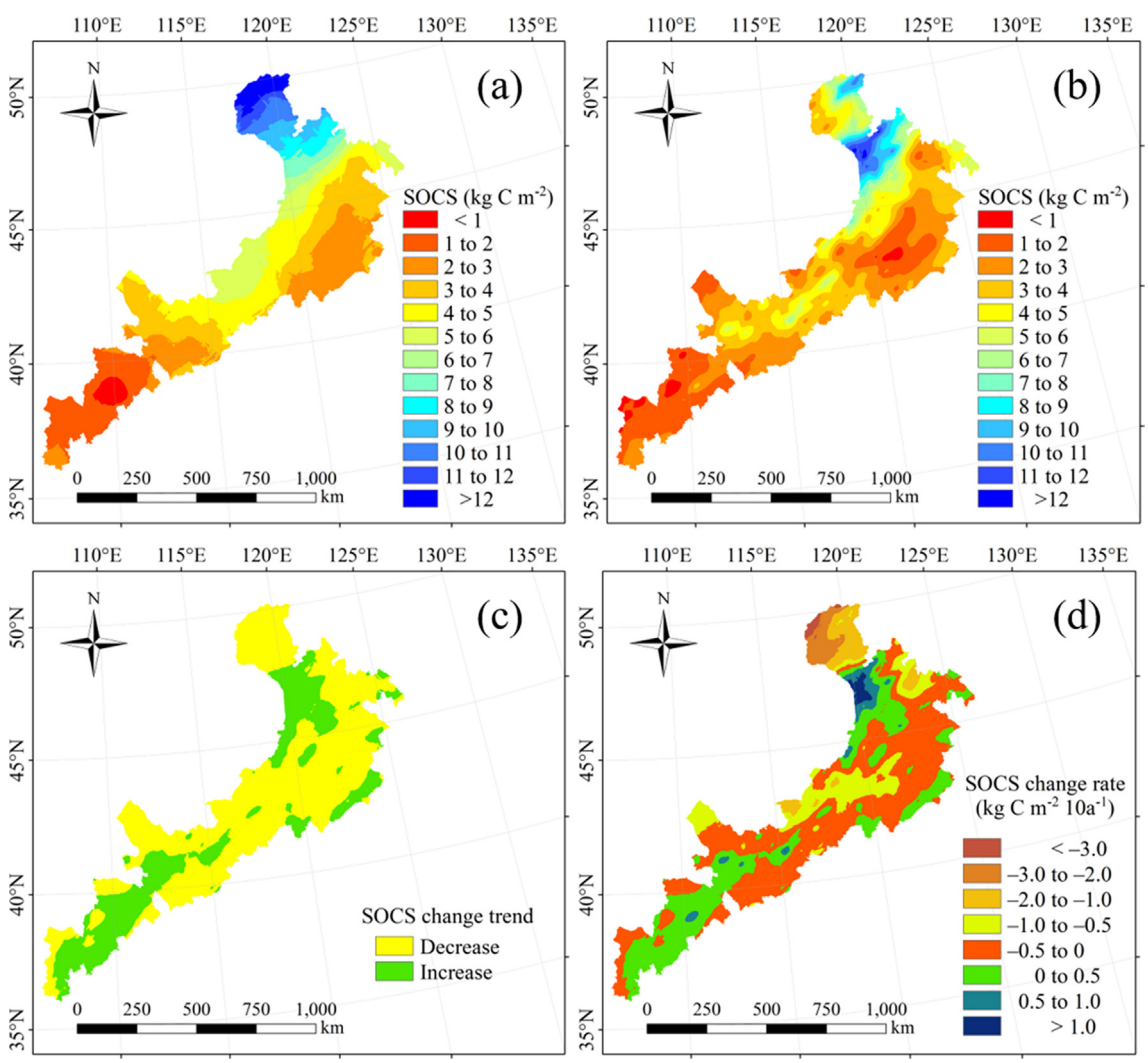

Fig. 3. Spatial patterns of the changes in soil organic carbon stock (*SOCS*) to a depth of 30 cm in (a) the 1980s and (b) 2018. (c) Change trends and (d) rate of change from the 1980s to 2018. Negative values represent decreases in *SOCS*.

Table 4
The soil organic carbon stock (*SOCS*) and total *SOCS* in the top 30 cm of the soil for the major land use and cover types in the study area, and the corresponding changes from the 1980s to 2018. *SOCS* values represent mean values ± standard deviations. Negative values represent decreases since the 1980 s. H-grassland, M−grassland, and L-grassland refer to grassland with high, medium, and low vegetation cover (i.e., more than 50%, 20% to 50%, and 5% to 20%, respectively).

Land use or cover type	1980s			2018			Changes (2018 value minus 1980s value)		
	Area (km^2)	*SOCS* (kg C m^{-2})	Total *SOCS* (Tg C)	Area (km^2)	*SOCS* (kg C m^{-2})	Total *SOCS* (Tg C)	Area (km^2)	*SOCS* (kg C m^{-2})	Total *SOCS* (Tg C)
Cropland	171,006	3.66 ± 1.84	625.60	187,298	3.26 ± 1.56	610.59	16,292	−0.40	−15.01
Forest	90,749	5.61 ± 2.67	508.83	102,992	5.12 ± 2.96	526.91	12,243	−0.49	18.08
H-grassland	119,997	5.33 ± 2.83	639.00	101,485	4.62 ± 2.38	469.01	−18512	−0.70	−169.98
M-grassland	117,785	4.87 ± 3.65	573.28	98,968	2.77 ± 1.50	273.66	−18817	−2.10	−299.62
L-grassland	45,827	3.28 ± 2.55	150.24	45,881	2.17 ± 0.99	99.74	54	−1.10	−50.49
Sandy land	30,187	2.38 ± 1.69	71.93	30,261	1.88 ± 1.09	57.03	74	−0.50	−14.90
Unused land	36,033	5.01 ± 3.00	180.57	38,817	3.94 ± 2.39	153.11	2784	−1.07	−27.46
Construction land	11,938	3.66 ± 1.54	43.73	18,669	3.12 ± 1.38	58.28	6731	−0.54	14.55
Total study area	623,522	4.48	2793.17	624,371	3.60	2248.34	—	−0.88	−544.83

3.4. Changes in SOCS and total SOCS between the 1980 s and 2018

The results of paired *t*-tests showed that *SOCS* decreased significantly from the 1980s to 2018 ($df = 881$, $t = 8.941$, $P < 0.001$). Mean *SOCS* from 882 sites was estimated to be 4.27 and 3.49 kg C m^{-2} for the 1980 s and the 2000 s, with 95% confidence intervals of 4.06 to 4.49 and 3.30 to 3.67 kg C m^{-2}, respectively (Table 3). SOC change over the 30-year study period amounted to −0.79 kg C m^{-2}, with 95% confidence interval of −0.98 to −0.59 kg C m^{-2}. Thus, SOC dynamics between 14% and 23% loss could not be detected by site-level comparison (Table 3).

Table 4 shows that for the whole study area, *SOCS* to a depth of 30 cm totaled 2793.17 Tg in the 1980 s and 2248.34 Tg C in 2018, with mean *SOCS* values of 4.48 and 3.60 kg C m^{-2}, respectively. The total *SOCS* decreased by 544.83 Tg, which amounted to an average decrease of 27.74 g C m^{-2} yr^{-1} during the 30-year study period. The *SOCS* in the top 30 cm of the soil for all land use and cover types decreased during the study period (Table 4). The M−grassland had the largest decrease, at 2.10 kg C m^{-2}, whereas cropland had the smallest decrease, at 0.40 kg C m^{-2}. The total *SOCS* showed the greatest decrease (520.09 Tg) for the total of the three types of grassland (H-grassland, M-grassland, and L-grassland), and this accounted for 95.5% of the total decrease in the total *SOCS*. The rates of decrease of the grassland total *SOCS* during the study period were in the following order (g C m^{-2} yr^{-1}): M-grassland (84.79) > H-grassland (47.22) > L-grassland (36.73). *SOCS* decreased most in the M-grassland (by 2.54 kg C m^{-2}). *SOCS* decreased by 0.09 kg C m^{-2} in cropland, whereas *SOCS* increased by 0.20 kg C m^{-2} in forest.

3.5. SOC changes caused by land-use conversion

During the 30 years covered by the present study, the conversion of sandy land to forest under the government's Three Norths Shelter Forest Program had the highest impact on the SOC sequestration potential, which increased by 2.73 kg C m^{-2} for the conversion of sandy land to forest. In contrast, *SOCS* decreased by 3.72 and 2.35 kg C m^{-2} for the conversion of forest to sandy land and cropland, respectively (Fig. 4). We further analyzed the conversions between land use and cover types between the 1980 s and 2018, and calculated the change of the total *SOCS* for different land use and cover type changes (Fig. 5). Specifically, for the areas in which the total *SOCS* increased, representing an increase of 64.8 Tg total *SOCS* in northern China's agro-pastoral ecotone, the contribution of afforestation was 53% (32% for cropland afforestation, 15% for grassland afforestation, and 6% for other activities), versus 40% for grassland construction (20% for returning cropland to grassland, 19% for planting grass in sandy land, and 1% for other activities). Of the total reduction of 544.83 Tg SOC, the contribution of grassland degradation or conversion to other uses was 61% (grassland degradation accounted for 37%, grassland reclamation for cropland accounted for 13%, grassland desertification accounted for 7%, and other activities accounted for 4%), whereas the contribution of forest degradation or conversion to other uses was 17%, and the contribution of cropland degradation or conversion was 12%.

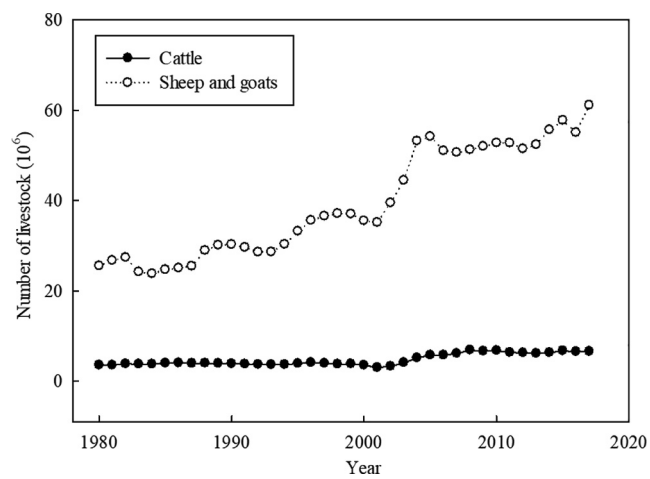

Fig. 4. Changes of soil organic carbon stock (*SOCS*) caused by different land use and cover type changes. Increases are shown as green bars, whereas decreases are shown as yellow bars. H-grassland, M-grassland, and L-grassland refer to grassland with high, medium, and low vegetation cover (i.e., more than 50%, 20% to 50%, and 5% to 20%, respectively).

3.6. The relationship between SOC and climate change

The Mann-Kendall test was used to detect significant trends in the annual temperature and precipitation from 1980 to 2015 in the study area. It was found that the annual average temperature increased significantly, at a rate of 0.36 °C·10 yr^{-1} in the past 30 years ($Z = 3.64$, $P < 0.01$), but that the annual precipitation did not change significantly, despite a decrease of 14.44 mm·10 yr^{-1} ($Z = -1.38$, $P > 0.05$) (Supplementary Figure S2). Almost the entire study area showed a warming trend, and only a small part of the eastern area showed a cooling trend (Fig. 6a). Furthermore, most of the study area showed decreasing precipitation, especially in the northern and eastern regions, but a small area showed an increasing trend in the southwestern region (Fig. 6b). Overall, the climate became warmer and drier in the entire study area. We performed regression analysis for the relationship between the change in *SOCS* and the rates of temperature and precipitation change. It was found that the increasing temperature non-significantly decreased *SOCS*, whereas increasing precipitation was significantly ($P < 0.05$) related to SOC change, but the R^2 was very

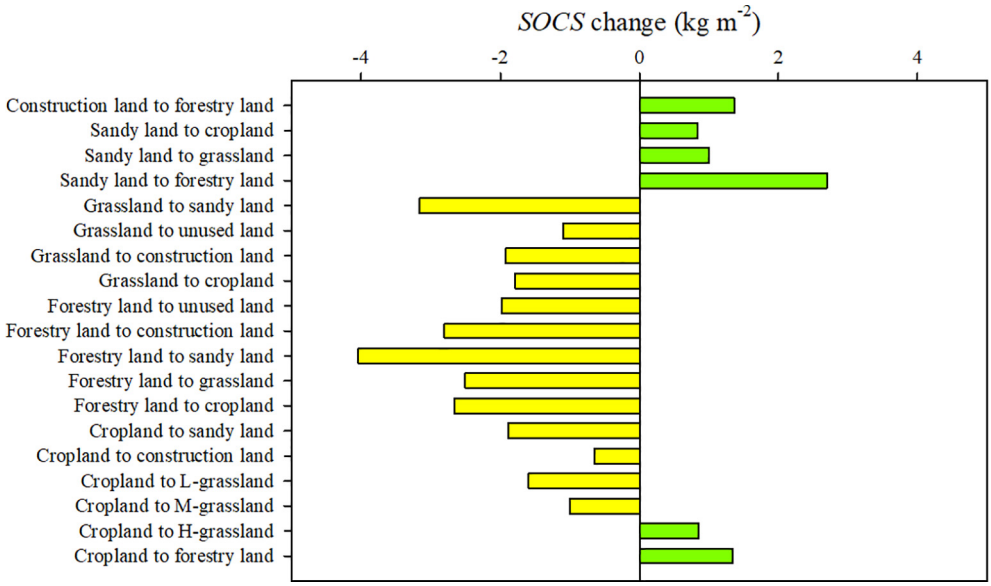

Fig. 5. Changes in the total soil organic carbon stock (*SOCS*) for different land use and cover type changes. Increases are shown as green bars, whereas decreases are shown as yellow bars. H-grassland, M-grassland, and L-grassland refer to grassland with high, medium, and low vegetation cover (i.e., more than 50%, 20% to 50%, and 5% to 20%, respectively). (For interpretation of the references to colour in this figure legend, the reader is referred to the web version of this article.)

low (0.01) (Fig. 7).

4. Discussion

4.1. SOCS for different land use and cover types

SOCS showed consistent relative values for each land use in the 1980 s and 2018. Forest and H-grassland showed high *SOCS* levels compared with other land uses in both periods, which can be attributed to the large amounts of aboveground biomass and abundant roots in these vegetation types, which promote the accumulation of *SOM* (Chang et al., 2012; Fu et al., 2010). In contrast, cropland had relatively low *SOCS*, mainly because the plant residues are removed during harvesting, resulting in low inputs of organic matter during the year (Wiesmeier et al., 2013). For grassland, there was a significant positive correlation between *SOCS* and vegetation cover, which was mainly attributed to the litter deposition caused by the increase of plant biomass, as a result of its benefit for the accumulation and retention of SOC (Jian et al., 2000; Xin et al., 2015). *SOCS* in the grassland of northern China's agro-pastoral ecotone (2.17 to 4.62 kg C m^{-2}) was lower than those in other regions, such as in the alpine meadow of Tibet (5.13 to 8.60 kg C m^{-2}), mainly because Tibet's cold climate inhibits the decomposition of *SOM*, resulting in an increase in SOC accumulation (Chen et al., 2017). Our values were also lower than the *SOCS* for grassland in Austria (10.7 kg·m^{-2}; Liski et al., 2012), Belgium (8.0 kg·m^{-2}; Meersmans et al., 2015), and Japan (11.4 kg·m^{-2}; Matsuura et al., 2012). A major cause of this difference is the widespread desertification that has occurred in northern China's degraded grasslands, and particular in the Mu Us Sandy Land, Horqin Sandy Land, and Hunshandake Sandy Land (Fig. 1b). Desertification directly decreases *SOCS* by eliminating many of the plants that are the source of SOC. The sandy land in our study area also experiences frequent wind erosion due to the high frequency of gale days. The severe wind erosion removes organic matter that has been provided as litter and removes fine particles from the topsoil, thereby decreasing the soil's ability to retain organic matter, resulting in the lowest *SOCS* in the sandy land (Lal, 1998; Li and Shao, 2014).

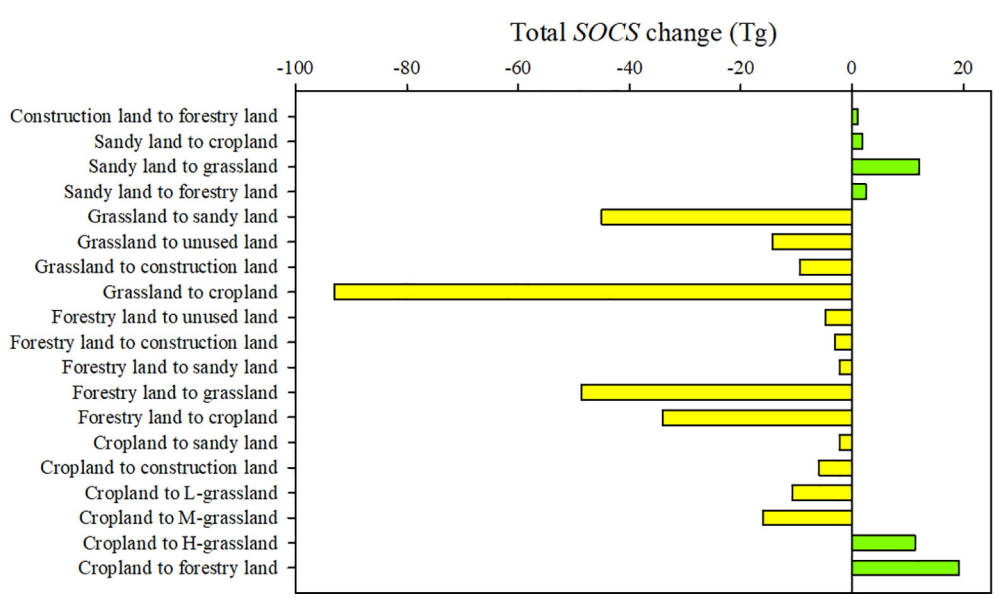

Fig. 6. Spatial distribution of the changes in (a) temperature and (b) precipitation per decade from 1980 to 2015 in northern China's agro-pastoral ecotone.

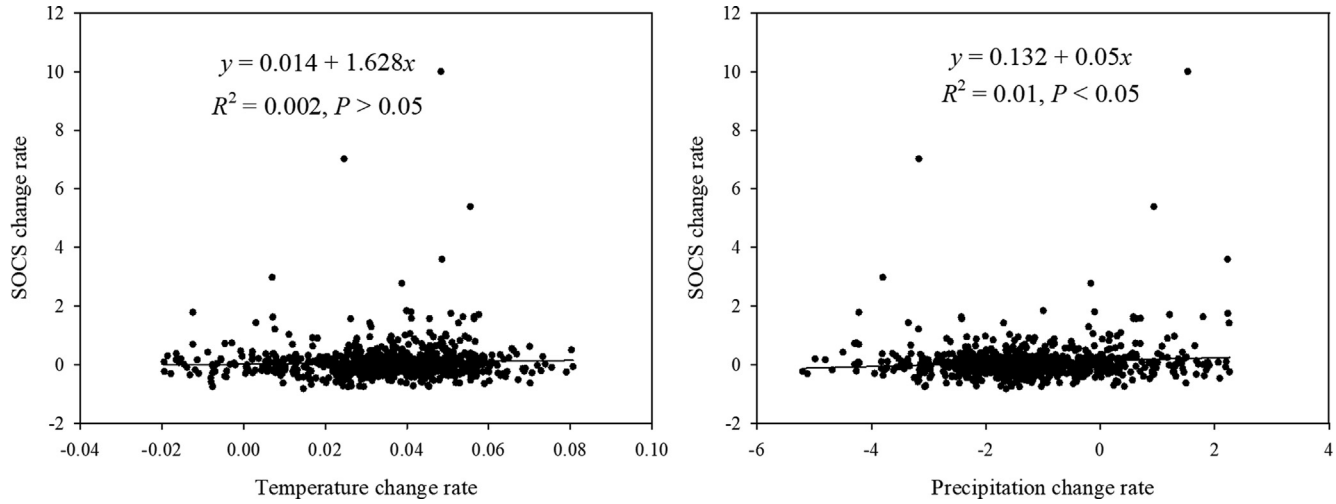

Fig. 7. The relationship between the change in soil organic carbon stock (*SOCS*) and the rates of (a) temperature and (b) precipitation change.

4.2. SOC changes between the 1980 s and 2018

In our research, the total *SOCS* to a depth of 30 cm in northern China's agro-pastoral ecotone decreased by 544.83 Tg C between the 1980 s and 2018. If we treat this decrease as a constant change, it amounted to an average decrease of 27.74 g C m^{-2} yr^{-1} during the 30-year study period. Our findings were consistent with the SOC change across England and Wales between 1978 and 2003, with a mean decrease of 31.4 g C m^{-2} yr^{-1} (Bellamy et al., 2005a, 2005b). The rates of decrease in grassland total *SOCS* were far greater than the decrease (0.60 g C m^{-2} yr^{-1}) in alpine grasslands of the Tibetan Plateau from the 1980 s to 2004 (Yang et al., 2009). This is mainly because in the alpine grasslands of the Tibetan Plateau, the increased soil C inputs due to increased grass productivity during the study period may have counteracted the loss of C associated with warming, resulting in a relatively stable total *SOCS*.

The total *SOCS* decreased at a rate of 27.74 g C m^{-2} yr^{-1} in northern China's agro-pastoral ecotone. In contrast, the total *SOCS* increased at a rate of 4.66 g C m^{-2} yr^{-1} from 2002 to 2011 in the alpine grasslands across the Tibetan Plateau (Chen et al., 2017). Furthermore, the topsoil (0 to 20 cm) total *SOCS* increased by 7.00 g C m^{-2} yr^{-1} in the grasslands of Inner Mongolia from 1982 to 2012 (Dai et al., 2014). These previous results are not consistent with our findings, in which the dramatic decrease in the grassland total *SOCS* resulted mainly from grassland degradation. The Inner Mongolia Autonomous Region is an important animal husbandry area in China, and accounted for 61.4% of the total study area (Fig. 1a). Changes in grazing pressure may explain our results. Taking the Inner Mongolia Autonomous Region as an example, the annual number of livestock (cattle, sheep, and goats) in the region from 1980 to 2017 (Fig. 8) were available from the National Bureau of Statistics of China (http://www.stats.gov.cn/tjsj/). Although the number of cattle remained relatively stable, the number of sheep and goats increased greatly, from 25.53 million animals in 1980 to 61.12 million in 2017. Furthermore, the area and quality of grassland have been decreasing since the 1980 s. The resulting long-term overgrazing decreased inputs of organic matter to the soil, resulting in a decreasing SOC content (Shi et al., 2009). The grassland in the agro-pastoral ecotone has also been seriously degraded by long-term overgrazing. Thus, the increasing grazing intensity is one of the major reasons for decreasing total *SOCS* in the study area. The discrepancies between the observations in our study and those of Dai et al. (2014) were mainly caused by different locations (Inner Mongolia accounted for only 61.4% of the present study area) and different grassland types. Dai et al. mainly studied natural grasslands in the central part of the Inner Mongolia Autonomous Region, which has been less affected by human activities and has retained relatively stable grassland vegetation during our study period. In contrast, the grasslands of northern China's agro-pastoral ecotone have been severely degraded by human activities (e.g., overgrazing).

The total *SOCS* of cropland decreased slightly, by 2.93 g C m^{-2} yr^{-1} in the present study, indicating that the SOC remained relatively stable compared with the other land use and cover types. This differs from the situation in Belgium, where the cropland total *SOCS* decreased at a rate of 608 kt C yr^{-1} in the 1990s in Belgium, mainly due to insufficient organic C inputs caused by reduced use of farmyard manure (Sleutel et al., 2010). In contrast, cropland in the United States showed an increasing total *SOCS* (1.3 Tg yr^{-1}) under the federally funded Conservation Reserve Program, which promoted the conversion of farmland into grassland (Ogle et al., 2010a,2010b), and as a result of decreased tillage intensity in the central United States (West et al., 2008). Liao et al. (2010) reported that the topsoil total *SOCS* (to a depth of 20 cm) in China's Jiangsu Province increased at a rate of 16.00 g C m^{-2} yr^{-1} between 1982 and 2004, mainly due to the increased agricultural production from paddy management. In the present study, which covers the period since China's reforms and opening up to the West under Deng Xiaoping, a massive migration of farmers to cities caused rural labor shortages, making it difficult to return large amounts of plant residues to the fields. Thus, farmers began to burn straw starting in the 1980s. Although Chinese farmers are more inclined to use large amounts of fertilizer to increase crop yields, thereby directly increasing inputs of organic matter to the soil, straw burning greatly reduced these inputs and decreased SOC accumulation (Zhao et al., 2018). Furthermore, most cropland in this region has been recently reclaimed from saline and alkaline lands in the vast North China Plain, where vegetation productivity is extremely low and organic C inputs are correspondingly low. This may explain the low level of current farmland SOC in the study area. Because the increasing burning of crop residues created severe air pollution, leading to closures of airports and highways in some areas, the Chinese government introduced a policy in 1999 to return crop residues to the field, which directly increased organic matter inputs to the soil (Gale, 2014). This compensated to some extent for the SOC loss that had been caused by straw burning. The combination of these factors led to relatively stable SOC from the 1980s to 2018 in the crop ecosystem of northern China's agro-pastoral ecotone.

4.3. Effects of land use change on SOC

The conversion of cropland to forest and H-grassland and the restoration of desertified land were the main factors responsible for

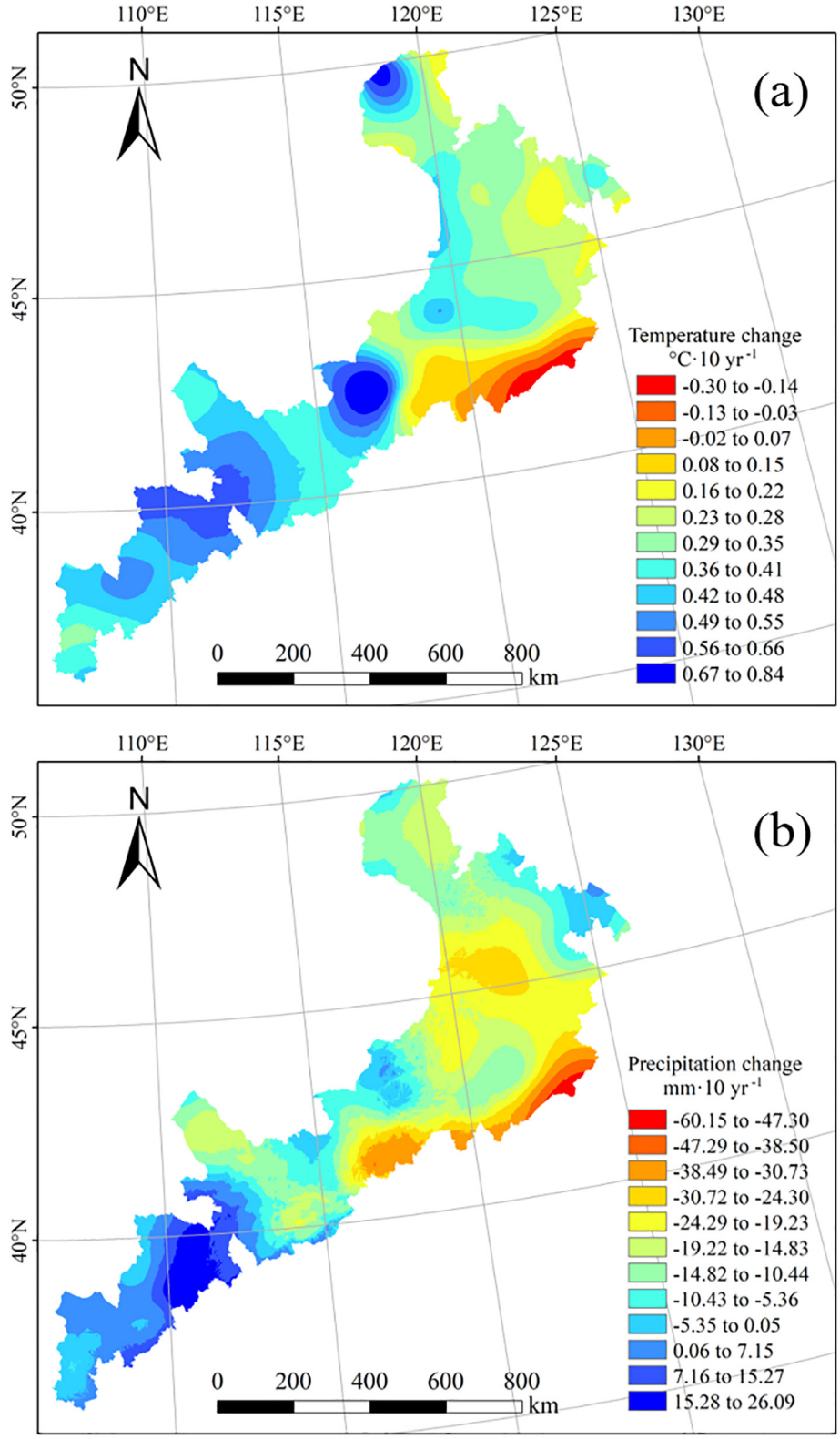

Fig. 8. Changes in the number of livestock (cattle, sheep, and goats) from 1980 to 2017 in China's Inner Mongolia Autonomous Region.

increases of the total *SOCS* in the study area, whereas grassland conversion to cropland and grassland degradation were the main factors responsible for decreases of *SOCS*. *SOCS* mainly benefited from the implementation of large-scale ecological protection projects, such as the national Three Norths Shelter Forest Program, which began in 1979, and a program to return farmland to forests and grassland, which began in 1999, as well as from other desertification control projects. These practices mainly included afforestation and grazing exclusion in northwestern, northern, and northeastern China.

4.4. Effects of climate change on SOC

Temperature and precipitation negatively and positively (respectively) affected *SOCS* because they affect the balance between carbon inputs from plant residues and carbon outputs caused by microbial decomposition of soil organic matter (Post et al., 1982). However, neither climate factor affected *SOCS* as strongly as anthropogenic land use change. We speculate that the accumulation of SOC caused by increasing precipitation would offset the losses of SOC caused by rising temperature; that is, the trend towards a warmer and drier climate would produce offsetting effects that weakened the impact of precipitation on SOC changes.

5. Conclusions

To better understand the current SOC reservoir and detect its changes over time in northern China's agro-pastoral ecotone, we conducted a field survey in 2018 to update the regional SOC information obtained during China's National Soil Inventory in the 1980 s. By comparing the measured *SOCS* in 2018 with the SOC values from the 1980 s, a large overall decline was found in *SOCS* to a depth of 30 cm, although the stock increased for forests and construction land due to (respectively) government afforestation programs and an increase in the area of construction land. The decreases could be mainly ascribed to overgrazing, grassland reclamation for agriculture, and grassland desertification. Large-scale ecological restoration projects have increased SOC reserves to a certain extent, but not by enough to compensate for the loss of SOC. In addition, the human influences on SOC change in northern China's agro-pastoral ecotone have been stronger than the climatic factors. The problem of grassland degradation is still serious. In the future, grassland protection and restoration should be strengthened in northern China's agro-pastoral ecotone to prevent further decreases in SOC.

Declaration of Competing Interest

None.

Acknowledgments

This research was supported by the National Key R and D Program of China (2017YFA0604803 and 2016YFC0500901), the National Natural Science Foundation of China (grants 31971466 and 41807525), and the One Hundred Person Project of the Chinese Academy of Sciences (Y551821).

Appendix A. Supplementary data

Supplementary data to this article can be found online at https://doi.org/10.1016/j.catena.2020.104722.

References

Allan Reese, R., 2001. Geostatistics for Environmental Scientists. John Wiley & Sons, 52 (3), 407.
Arrouays, D., Deslais, W., Badeau, V., 2010. The carbon content of topsoil and its geographical distribution in France. Soil Use Manage. 17 (1), 7–11. https://doi.org/10.1111/j.1475-2743.2001.tb00002.x.
Arrouays, D., Jolivet, C., Boulonne, L., Bodineau, G., Saby, N., Grolleau, E., 2002. A new projection in France: A multi-institutional soil quality monitoring network. Comptes Rendus de l' Académie d' agriculture de France. 88, 93–103.
Batjes, N.H., 2000. Effects of mapped variation in soil conditions on estimates of soil carbon and nitrogen stocks for South America. Geoderma. 97 (1–2), 135–144. https://doi.org/10.1016/s0016-7061(00)00031-8.
Batjes, N.H., 2014. Total carbon and nitrogen in the soils of the world. Eur. J. Soil Sci. 65 (1), 10–21. https://doi.org/10.1111/ejss.12114_2.
Beilman, D.W., Vitt, D.H., Bhatti, J.S., Forest, S., 2008. Peat carbon stocks in the southern Mackenzie River Basin: uncertainties revealed in a high-resolution case study. Global Change Biol. 14, 1221–1232.
Bell, M.J., Worrall, F., Smith, P., Bhogal, A., Merrington, G., 2011. UK land-use change and its impact on SOC: 1925–2007. Global Biogeochem. Cyc. 25 (4), 4015.
Bellamy, P.H., Loveland, P.J., Bradley, R.I., Lark, R.M., Kirk, G.J.D., 2005. Carbon losses from all soils across England and Wales 1978–2003. Nature 437, 245–248. https://doi.org/10.1038/nature04038.
Bellamy, P.H., Loveland, P.J., Bradley, R.I., Lark, R.M., Kirk, G.J.D., 2005b. Carbon losses from all soils across England and Wales 1978–2003. Nature. 437 (7056), 245–248. https://doi.org/10.1038/nature04038.
Bernoux, M., Sant, M.D.C., Volkoff, B., Cerri, C.C., 2002. Brazil's soil carbon stocks. Soil Sci. Soc. Am. J. 66 (3), 888–896. https://doi.org/10.2136/sssaj2002.8880.
Bhattacharyya, T., Pal, D.K., Mandal, C., Velayutham, M., 2000. Organic carbon stock in Indian soils and their geographical distribution. Curr. Sci. 79 (5), 655–660. https://doi.org/10.1073/pnas.180319797.
Cambardella, C.A., Moorman, T.B., Parkin, T.B., Karlen, D.L., Novak, J.M., Turco, R.F., Konopka, A.E., 1994. Field-scale variability of soil properties in central Iowa soils. Soil Sci. Soc. Am. J. 58 (5), 1501–1511.
Capriel, P., 2013. Trends in organic carbon and nitrogen contents in agricultural soils in Bavaria (south Germany) between 1986 and 2007. Eur. J. Soil Sci. 64 (4), 445–454. https://doi.org/10.1111/ejss.12054.
Chang, R., Fu, B., Liu, G., Shuai, W., Yao, X., 2012. The effects of afforestation on soil organic and inorganic carbon: A case study of the Loess Plateau of China. Catena. 95 (3), 145–152. https://doi.org/10.1016/j.catena.2012.02.012.
Chen, L., Xin, J., Dan, F.B.F., Yue, S., Kühn, P., Scholten, T., He, J.S., 2017. Changes of carbon stocks in alpine grassland soils from 2002 to 2011 on the Tibetan Plateau and their climatic causes. Geoderma. 288, 166–174. https://doi.org/10.1016/j.geoderma.2016.11.016.
Dai, E., Zhai, R., Ge, Q., Wu, X., 2014. Detecting the storage and change on topsoil organic carbon in grasslands of Inner Mongolia from 1980s to 2010s. J. Geog. Sci. 24 (6), 1035–1046. https://doi.org/10.1007/s11442-014-1136-9.
Davidson, E.A., Janssens, I.A., 2006. Temperature sensitivity of soil carbon decomposition and feedbacks to climate change. Nature. 440 (7081), 165–173. https://doi.org/10.1038/nature04514.
Deng, L., Shangguan, Z., 2017. Afforestation drives soil carbon and nitrogen changes in China. Land Degrad. Devel. 28, 151–165.
Eswaran, H., Vandenberg, E., Reich, P., 1993. Organic carbon in soils of the world. Soil Sci. Soc. Am. J. 57 (1), 192–194. https://doi.org/10.2136/sssaj1993.03615995005700010034x.
Fu, X., Shao, M., Wei, X., Horton, R., 2010. Soil organic carbon and total nitrogen as affected by vegetation types in Northern Loess Plateau of China. Geoderma. 155 (1), 31–35. https://doi.org/10.1016/j.geoderma.2009.11.020.
Gale, F., 2014. Growth and evolution in China's agricultural support policies. Economic Research Report from United States Department of Agriculture, Economic Research Service, no. 155385. Available at http://ageconsearch.umn.edu/record/155385/files/err153.pdf.
Gelaw, A.M., Singh, B.R., Lal, R., 2014. Soil organic carbon and total nitrogen stocks under different land uses in a semi-arid watershed in Tigray, Northern Ethiopia. Agric. Ecosyst. Environ. 188 (15), 256–263. https://doi.org/10.1016/j.agee.2014.02.035.
Ingram, J.S.I., Fernandes, E.C.M., 2001. Managing carbon sequestration in soils: concepts and terminology. Agric Ecosyst Environ. 87 (1), 111–117. https://doi.org/10.1016/S0167-8809(01)00145-1.
Jian, R.W., Letchford, T., Comeau, P., Kimmins, J.P., 2000. Above- and below-ground biomass and nutrient distribution of a paper birch and subalpine fir mixed-species stand in the Sub-Boreal Spruce zone of British Columbia. For. Ecol. Manage. 130 (1), 17–26. https://doi.org/10.1016/S0378-1127(99)00193-0.
Jobbagy, E.G., Jackson, R.B., 2000. The vertical distribution of soil organic carbon and its relation to climate and vegetation. Ecol. Appl. 10 (2), 423–436. https://doi.org/10.2307/2641104.
Klute, A., 1986. Methods of soil analysis. Part 1. Physical and mineralogical methods. Methods Soil Anal. Part. Phys. Mineral. Methods 146 (2), 413–423. https://doi.org/10.2136/sssabookser5.1.2ed.c15.
Krogh, L., Noergaard, A., Hermansen, M., Greve, M.H., Balstroem, T., Breuning-Madsen, H., 2003. Preliminary estimates of contemporary soil organic carbon stocks in Denmark using multiple datasets and four scaling-up methods. Agric. Ecosyst. Environ. 96 (1), 19–28. https://doi.org/10.1016/S0167-8809(03)00016-1.
Lal, R., 1998. Soil erosion impact on agronomic productivity and environment quality. Crit. Rev. Plant Sci. 17 (4), 319–464. https://doi.org/10.1080/07352689891304249.
Lal, R., 2001. Potential of desertification control to sequester carbon and mitigate the greenhouse effect. Clim. Change. 51 (1), 35–72. https://doi.org/10.1023/A:1017529816140.
Lal, R., 2004. Soil carbon sequestration to mitigate climate change. Geoderma. 123, 1–22.
Li, Y.Q., Chen, Y.P., Wang, X.Y., Niu, Y.Y., Lian, J., 2017. Improvements in soil carbon and nitrogen capacities after shrub planting to stabilize sand dunes in China's Horqin Sandy Land. Sustainability 9, 662.
Li, D., Shao, M.A., 2014. Soil organic carbon and influencing factors in different landscapes in an arid region of northwestern China. Catena. 116 (116), 95–104. https://doi.org/10.1016/j.catena.2013.12.014.
Li, Y.Q., Wang, X.Y., Niu, Y.Y., Jie, L., Luo, Y.Q., Chen, Y.P., Gong, X.W., Yang, H., Yu, P.D., 2018. Spatial distribution of soil organic carbon in the ecologically fragile Horqin Grassland of northeastern China. Geoderma. 325, 102–109. https://doi.org/10.1016/j.geoderma.2018.03.032.
Li, Y.Q., Brandle, J., Awada, T., Chen, Y.P., Han, J.J., Zhang, F., Luo, Y.Q., 2013. Accumulation of carbon and nitrogen in the plant-soil system after afforestation of active sand dunes in China's Horqin Sandy Land. Agric. Ecosyst. Environ. 177, 75–84.
Liao, Q.L., Zhang, X.H., Li, Z.P., Pan, G.X., Smith, P., Yang, J., Wu, X.M., 2010. Increase in soil organic carbon stock over the last two decades in China's Jiangsu Province.

Global Change Biol. 15 (4), 861–875. https://doi.org/10.1111/j.1365-2486.2008.01792.x.
Liski, J., Perruchoud, D., Karjalainen, T., 2012. Increasing carbon stocks in the forest soils of western Europe. For. Ecol. Manage. 169 (1), 159–175. https://doi.org/10.1016/S0378-1127(02)00306-7.
Liu, Z., Li, L.T., McVicar, T.R., van Niel, T.G., Yang, Q.K., Li, R., 2008. Introduction of the professional interpolation software for meteorology data:ANUSPLINN. Meteorol. Mon. 34 (2), 92–100.
Mann, H.B., 1945. Nonparametric tests against trend. Econometrica. 13, 245–259.
Martin, M.P., Orton, T.G., Lacarce, E., Meersmans, J., Saby, N.P.A., Paroissien, J.B., Jolivet, C., Boulonne, L., Arrouays, D., 2014. Evaluation of modelling approaches for predicting the spatial distribution of soil organic carbon stocks at the national scale. Geoderma 223–225 (1), 97–107. https://doi.org/10.1016/j.geoderma.2014.01.005.
Matsuura, S., Sasaki, H., Kohyama, K., 2012. Organic carbon stocks in grassland soils and their spatial distribution in Japan. Grassland Sci. 58 (2), 79–93. https://doi.org/10.1111/j.1744-697X.2012.00245.x.
Meersmans, J., Wesemael, B.V., Goidts, E., Molle, M.V., Baets, S.D., Ridder, F.D., 2015. Spatial analysis of soil organic carbon evolution in Belgian croplands and grasslands, 1960–2006. Global Change Biol. 17 (1), 466–479. https://doi.org/10.1111/j.1365-2486.2010.02183.x.
Minasny, B., Sulaeman, Y., Mcbratney, A.B., 2011. Is soil carbon disappearing? The dynamics of soil organic carbon in Java. Global Change Biol. 17 (5), 1917–1924. https://doi.org/10.1111/j.1365-2486.2010.02324.x.
Nelson, D.W., Sommers, L.E., Sparks, D.L., Page, A.L., Helmke, P.A., Loeppert, R.H., Sumner, M.E., 1996. Total carbon, organic carbon, and organic matter. Methods Soil Anal. 9, 961–1010. https://doi.org/10.2136/sssabookser5.3.c34.
Nosetto, M.D., Jobbágy, E.G., Paruelo, J.M., 2006. Carbon sequestration in semi-arid rangelands: Comparison of Pinus ponderosa plantations and grazing exclusion in NW Patagonia. J. Arid. Environ. 67 (1), 142–156. https://doi.org/10.1016/j.jaridenv.2005.12.008.
Novaes, R.M.L., Pazianiotto, R.A.A., Brandaã, M., Alves, B.J.R., May, A., Folegatti-Matsuura, M.I.S., 2017. Estimating 20-year land-use change and derived CO_2 emissions associated with crops, pasture and forestry in Brazil and each of its 27 states. Global Change Biol. 23 (9), 3716–3728. https://doi.org/10.1111/gcb.13708.
Ogle, S.M., Breidt, F.J., Easter, M., Williams, S., Killian, K., Paustian, K., 2010a. Scale and uncertainty in modeled soil organic carbon stock changes for US croplands using a process-based model. Global Change Biol. 16 (2), 810–822. https://doi.org/10.1111/j.1365-2486.2009.01951.x.
Ogle, S.M., Breidt, F.J., Eve, M.D., Paustian, K., 2003. Uncertainty in estimating land use and management impacts on soil organic carbon storage for US agricultural lands between 1982 and 1997. Global Change Biol. 9, 1521–1542.
Ogle, S.M., Breidt, F.J., Eve, M.D., Paustian, K., 2010b. Uncertainty in estimating land use and management impacts on soil organic storage for US agricultural lands between 1982 and 1997. Global Change Biol. 9 (11), 1521–1542. https://doi.org/10.1046/j.1365-2486.2003.00683.x.
Post, W.M., Emanuel, W.R., Zinke, P.J., Stangenberger, A.G., 1982. Soil carbon pools and world life zones. Nature. 298 (5870), 156–159. https://doi.org/10.1038/298156a0.
Potvin, C., Roff, D.A., 1993. Distribution-free and robust statistical methods: viable alternatives to parametric statistics. Ecology. 74, 1617–1628. https://doi.org/10.2307/1939920.
Pribyl, D.W., 2010. A critical review of the conventional SOC to SOM conversion factor. Geoderma 156 (3–4), 0–83. https://doi.org/10.1016/j.geoderma.2010.02.003.
R Development Core Team. R: A Language and Environment for Statistical Computing. R Foundation for Statistical Computing, Vienna, Austria, 2008 http://www.R-project.org.
Raich, J.W., Potter, C.S., 1995. Global patterns of carbon dioxide emissions from soils. Global Biogeochem. Cycles. 9 (1), 23–36. https://doi.org/10.1029/94GB02723.
Scharlemann, J.P., Tanner, E.V., Hiederer, R., Kapos, V., 2014. Global soil carbon: understanding and managing the largest terrestrial carbon pool. Carbon Manage. 5 (1), 81–91. https://doi.org/10.4155/cmt.13.77.
Schlesinger, W.H., 1990. Evidence from chronosequence studies for a low carbon-stock potential of soils. Nature. 348 (6298), 232–234. https://doi.org/10.1038/348232a0.
Schlesinger, W.H., 2001. Carbon sequestration in soils: some cautions amidst optimism. Agric. Ecosyst. Environ. 82 (1), 121–127. https://doi.org/10.1016/s0167-8809(00)00221-8.
Sheikh, M.A., Kumar, M., Bussmann, R.W., 2009. Altitudinal variation in soil organic carbon stock in coniferous subtropical and broadleaf temperate forests in Garhwal Himalaya. Carbon Balance Manage. 4 (1), 6. https://doi.org/10.1186/1750-0680-4-6.
Shi, F., Li, Y.E., Gao, Q.Z., Wan, Y.F., Qin, X.B., Jin, L., Liu, Y.T., Wu, Y.J., 2009. Effects of managements on soil organic carbon of grassland in China. Pratacultural Sci. 26 (3), 9–15.
Shi, X.Z., Yu, D.S., Warner, E.D., Pan, X.Z., Petersen, G.W., Gong, Z.G., Weindorf, D.C., 2004. Soil database of 1:1,000,000 digital soil survey and reference system of the Chinese genetic soil classification system. Soil Survey Horizons 45 (4), 129. https://doi.org/10.2136/sh2004.4.0129.
Sleutel, S., Neve, S.D., Hofman, G., 2010. Estimates of carbon stock changes in Belgian cropland. Soil Use Manage. 19 (2), 166–171. https://doi.org/10.1111/j.1475-2743.2003.tb00299.x.
Smith, P., Fang, C., Dawson, J.J.C., Moncrieff, J.B., 2008. Impact of global warming on soil organic carbon. In: Sparks, D.L. (Ed.), Advances in Agronomy. 97, 1-43. doi: 10.1016/S0065-2113(07)00001-6.
Smith, P., Smith, J.U., Powlson, D.S., Mcgill, W.B., Arah, J.R.M., Chertov, O.G., Jenkinson, D.S., 1997. A comparison of the performance of nine soil organic matter models using datasets from seven long-term experiments. Geoderma. 81 (1–2), 153–225. https://doi.org/10.1007/BF02704837.
Su, Y.Z., Zhao, H.L., Zhang, T.H., 2003. Influence of grazing and exclosure on carbon sequestration in degraded sandy grassland, Inner Mongolia, north China. N. Z. J. Agric. Res. 46, 321–328.
Tashi, S., Singh, B., Keitel, C., Adams, M., 2016. Soil carbon and nitrogen stocks in forests along an altitudinal gradient in the eastern Himalayas and a meta-analysis of global data. Global Change Biol. 22 (6), 2255–2268. https://doi.org/10.1111/gcb.13234.
Valtera, M., Šamonil, P., 2018. Soil organic carbon stocks and related soil properties in a primary Picea abies (L.) Karst. volcanic-mountain forest. Catena. 165, 217–227. https://doi.org/10.1016/j.catena.2018.01.034.
Vandenbygaart, A.J., Gregorich, E.G., Angers, D.A., Stoklas, U.F., 2004. Uncertainty analysis of soil organic carbon stock change in Canadian cropland from 1991 to 2001. Global Change Biol. 10, 983–994.
Wan, J., Zhang, H.Y., Wang, J.N., Cha zhong, G.E., Gao, S.T., 2005. Policy evaluation and framework discussion of ecological compensation mechanism in China. Res. Environ. Sci. 18(2), 1-8. (in Chinese).
Wang, X.M., Zhang, C.X., Hasi, E., Dong, Z.B., 2010. Has the Three Norths Forest Shelterbelt Program solved the desertification and dust storm problems in arid and semiarid China? J. Arid. Environ. 74 (1), 13–22.
Wang, X.Y., Li, Y.Q., Gong, X.W., Niu, Y.Y., Chen, Y.P., Shi, X.P., 2019. Storage, pattern and driving factors of soil organic carbon in an ecologically fragile zone of northern China. Geoderma. 343, 155–165.
Wang, Y., Deng, L., Wu, G., Wang, K., Shangguan, Z., 2018. Estimates of carbon storage in grassland ecosystems on the Loess Plateau. Catena. 164, 23–31. https://doi.org/10.1016/j.catena.2018.01.007.
Were, K., Bui, D.T., Dick, Ø.B., Singh, B.R., 2015. A comparative assessment of support vector regression, artificial neural networks, and random forests for predicting and mapping soil organic carbon stocks across an Afromontane landscape. Ecol. Indic. 52, 394–403. https://doi.org/10.1016/j.ecolind.2014.12.028.
West, T.O., Brandt, C.C., Marland, G., Ugarte, D.G.D.L.T., Larson, J.A., Hellwinckel, C.M., Nelson, R.G., 2008. Estimating regional changes in soil carbon with high spatial resolution. Soil Sci. Soc. Am. J. 72 (2), 285–294. https://doi.org/10.2136/sssaj2007.0113.
Wiesmeier, M., Hübner, R., Barthold, F., Spörlein, P., Geuß, U., Hangen, E., Kögel-Knabner, I., 2013. Amount, distribution and driving factors of soil organic carbon and nitrogen in cropland and grassland soils of southeast Germany (Bavaria). Agric. Ecosyst. Environ. 176 (1765), 39–52. https://doi.org/10.1016/j.agee.2013.05.012.
Xin, Z., Qin, Y., Yu, X., 2015. Spatial variability in soil organic carbon and its influencing factors in a hilly watershed of the Loess Plateau. China. Catena. 137, 660–669. https://doi.org/10.1016/j.catena.2015.01.028.
Yang, Y.H., Fang, J.Y., Ma, W., Smith, P., Mohammat, A., Wang, S., Wang, W., 2010a. Soil carbon stock and its changes in northern China's grasslands from 1980s to 2000s. Global Change Biol. 16 (11), 3036–3047. https://doi.org/10.1111/j.1365-2486.2009.02123.x.
Yang, Y.H., Fang, J.Y., Smith, P., Tang, Y.H., Chen, A.P., Ji, C.J., Hu, H.F., Rao, S., Tan, K., He, J.S., 2009. Changes in topsoil carbon stock in the Tibetan grasslands between the 1980s and 2004. Global Change Biol. 15 (11), 2723–2729. https://doi.org/10.1111/j.1365-2486.2009.01924.x.
Yang, Y.H., Mohammat, A., Feng, J., Zhou, R., Fang, J., 2007. Storage, patterns and environmental controls of soil organic carbon in China. Biogeochemistry. 84 (2), 131–141. https://doi.org/10.1007/s10533-007-9109-z.
Yang, Y., Fang, J., Ma, W., Smith, P., Mohammat, A., Wang, S., Wang, W., 2010b. Soil carbon stock and its changes in northern China's grasslands from 1980s to 2000s. Global Change Biol. 16 (11), 3036–3047.
Zhang, T.H., Zhao, H.L., Li, S.G., Li, F.R., Shirato, Y., Ohkuro, T., Taniyama, I., 2004. A comparison of different measures for stabilizing moving sand dunes in the Horqin Sandy Land of Inner Mongolia, China. J. Arid Environ. 58, 203–214.
Zhao, H.L., Zhao, X.Y., Zhang, T.H., Zhou, R.L., 2002. Boundary line on agro-pasture zigzag zone in north China and its problems on eco-environment. Adv. Earth Sci. 17 (5), 739–747. https://doi.org/10.1007/s11769-002-0041-9. in Chinese.
Zhao, Y.C., Wang, M.Y., Hu, S.J., Zhang, X.D., Ouyang, Z., Zhang, G.L., Huang, B., Zhao, S.W., Wu, J.S., Xie, D.T., Zhu, B., Yu, D.S., Pan, X.Z., Xu, S.X., Shi, X.Z., 2018. Economics- and policy-driven organic carbon input enhancement dominates soil organic carbon accumulation in Chinese croplands. Proc. Natl. Acad. Sci. U.S.A. 115 (16), 4045. https://doi.org/10.1073/pnas.1700292114.